Anomalous behavior of the internal stretching modes above and below the incommensurate phase transition of Cs$_2$HgBr$_4$

A. Jório, M. S. S. Dantas, C. B. Pinheiro, N. L. Speziali, and M. A. Pimenta

Departamento de Física, Universidade Federal de Minas Gerais, C. P. 702, 30123-970, Belo Horizonte, Minas Gerais, Brazil

A Raman study of Cs$_2$HgBr$_4$ crystals was performed in the temperature range 90–290 K, using different scattering geometries. A high-resolution analysis of the bands associated with the stretching vibrations of the HgBr$_4^{-2}$ tetrahedra reveals that the frequency of the peak associated with the A_g symmetry ν_1 mode observed in the (xx) spectrum is smaller than those observed in the (yy) and (zz) spectra. The temperature dependence of this frequency shift shows a discontinuous decrease at the incommensurate phase transition T_I and a jump to zero at lower temperature. This result is interpreted in terms of the orientational disorder of the HgBr$_4^{-2}$ groups. Besides, a TO-LO splitting appears at T_I, increases continuously in the incommensurate phase, and remains constant below the lock-in phase transition. This result is in disagreement with the centrosymmetric structures proposed for the low-temperature phases and is probably due to the presence of a layered structure of domain walls with polar symmetry. [S0163-1829(97)07246-9]

I. INTRODUCTION

Crystals of the family A_2BX_4 have been the object of many experimental and theoretical studies in the last years, due to the existence of a large variety of structural phases. The richness of the structural phases is related to the existence of orientational disorder of the BX_4 sublattice at high temperature and different possible orientations of the BX_4 tetrahedra when temperature decreases. In particular, some crystals of this family exhibit incommensurate phases, where the angle of rotation of the BX_4 tetrahedra is modulated along a given direction. The most studied of them, e.g., K$_2$SeO$_4$, Rb$_2$ZnCl$_4$, Rb$_2$ZnBr$_4$, K$_2$ZnCl$_4$, etc., present the same sequence of phase transition, that is, a high-temperature phase belonging to the $Pnma$ space group, an incommensurate structure where the modulation wave vector presents a temperature dependence given by $q(T) = n/m[1 + \delta(T)]a^*$, and a lock-in (or commensurate) m-fold superstructure belonging to the $Pn2_1a$ space group. The high-temperature structure, above the incommensurate phase transition at T_I, is also characterized by an orientational disorder of the BX_4 tetrahedra, the extent of disorder varying from one compound to another.

Cs$_2$HgBr$_4$ crystals also exhibit an incommensurate phase at low temperature, but their structural behavior below T_I is different from the well-known K$_2$SeO$_4$-type incommensurate compounds. The high-temperature structure (phase I) belongs to the $Pnma$ (D_{2h}^{16}, $Z=4$) space group, but the incommensurate phase (phase II) below $T_I = 245$ K is characterized by a wave vector $\mathbf{q} \approx 0.16a^*$ that practically does not change in the whole incommensurate interval. At about $T_C = 232$ K, the modulation wave vector jumps to zero, yielding a commensurate structure (phase III) belonging to the monoclinic space group $P2_1/n$ (C_{2h}^5, $Z=4$), without the appearance of a superstructure. The crystal undergoes two other phase transitions, at about $T_{L1} = 165$ K and $T_{L2} = 80$ K. Phase IV (80 K $< T <$ 165 K) belong to the triclinic space group $P\bar{1}$ (C_i^1, $Z=4$) and phase V ($T < 80$ K) belong to the same group, with $Z=8$.[1]

Different experimental techniques have been used to study the sequence of phase transitions of Cs$_2$HgBr$_4$, like x-ray diffraction,[2,3] NQR,[2–5] NMR,[6] optical birefringence,[3,7–10] acoustical studies,[10] specific heat,[11] and Raman scattering.[12] Besides the appearance of satellite spots in the x-ray-diffraction patterns, the incommensurate phase, between $245 > T > 232$ K, was also characterized by the broad NMR and NQR bands.

Dmitriev *et al.*[12] performed a Raman study of Cs$_2$HgBr$_4$ between 100 and 300 K using different scattering geometries. They focused their attention on the low-frequency region of the spectrum, which corresponds to the external modes of the crystal. At very low frequency they observed a relaxation mode with a characteristic time $\tau \approx 5 \times 10^{-13}$ s, which was ascribed to the existence of a small-angle orientational jump of the HgBr$_4^{-2}$ groups. According to them, the orientational disorder of the HgBr$_4^{-2}$ groups is present in phases I, II, and III, and disappears in phase IV, below $T_{L1} = 165$ K.

In this work, we study the high-frequency region of the spectra which corresponds to the internal stretching modes of the HgBr$_4^{2-}$ tetrahedra. Raman spectra were obtained using different scattering geometries and different phonon propagation directions, between 90 and 290 K. The high-resolution of the spectra allowed us to perform a careful line-shape analysis of the bands associated with the internal stretching modes, revealing new aspects of the transitional behavior above and below the incommensurate phase transition.

II. EXPERIMENT

Single colorless crystals of Cs$_2$HgBr$_4$ were grown by H. Arend (ETH, Zurich) using the Bridgman method. We have used the convention for the orthorhombic crystal axes in which a is the pseudohexagonal axis and $b < a < c$ (a

TABLE I. Correlation diagram for the internal modes in the room-temperature phase I of Cs_2HgBr_4.

point group of the free molecule	site group	factor group	internal modes
T_d	σ_y	D_{2h}	
A_1 (ν_1)		A_g (x^2, y^2, z^2)	$\nu_1, \nu_2, 2\nu_3, 2\nu_4$, lib, 2ext
		B_{1g} (yz)	ν_2, ν_3, ν_4, 2lib, ext
E (ν_2)	A	B_{2g} (xy)	ν_2, ν_3, ν_4, 2lib, ext
		B_{3g} (xz)	$\nu_1, \nu_2, 2\nu_3, 2\nu_4$, lib, 2ext
T_1 (lib.)	B	A_u	ν_2, ν_3, ν_4, 2lib, ext
		B_{1u} (x)	$\nu_1, \nu_2, 2\nu_3, 2\nu_4$, lib, 2ext
T_2 (ν_3, ν_4, ext.)		B_{2u} (z)	$\nu_1, \nu_2, 2\nu_3, 2\nu_4$, lib, 2ext
		B_{3u} (y)	ν_2, ν_3, ν_4, 2lib, ext

$= 10.248$ Å, $b = 7.927$ Å, and $c = 13.901$ Å),[4] in accordance with the *Pnma* space group for the structure at room temperature.[13] The c axes is perpendicular to an easy cleavage plane of the crystal. The samples were cut and polished with the faces perpendicular to the crystallographic axes.

The Raman spectra have been recorded with a triple-monochromator spectrometer (DILOR *XY*) equipped with a multiarray detector (GOLD) and excited with a 150 mW green line ($\lambda = 514.5$ nm) of an argon laser (COHERENT INNOVA 70). A flow cold-finger cryostat (Janis ST-300) and a temperature controller (LakeShore 330) allowing a temperature stability better than 0.1 K were used for the low-temperature experiments.

We have used nine different backscattering configurations to observe all modes belonging to all Raman-active representations and propagating along different directions, that is, $x(yy)\bar{x}$, $x(zz)\bar{x}$, $x(yz)\bar{x}$, $y(xx)\bar{y}$, $y(zz)\bar{y}$, $y(xz)\bar{y}$, $z(xx)\bar{z}$, $z(yy)\bar{z}$, $z(xy)\bar{z}$. The symbols inside the parentheses give the polarization of the incident and scattered light and the symbols outside the parenthesis give the phonon propagation directions.

III. GROUP THEORY ANALYSIS

The present analysis is restricted to the internal vibrational modes of the $HgBr_4^{2-}$ anions in phases I–IV. Tables I, II, and III show the factor-group analysis for the normal phases I, III, and IV, respectively. The unit cell contains four $HgBr_4^{2-}$ tetrahedra and thus there are 36 internal modes ($4\nu_1, 8\nu_2, 12\nu_3, 12\nu_4$). Since all the point groups are centrosymmetric, only the 18 internal modes associated with the gerade irreducible representation are Raman active and, therefore, their frequencies should not depend on the direction of propagation. The quadratic functions, which give the scattering polarization used to observe the modes associated with each representation, are also presented in these tables. The functions xx, yy, and zz always belong to the A_g representation.

At the room temperature phase I (*Pnma* or D_{2h}^{16} space group), the $HgBr_4^{2-}$ tetrahedra are localized, on average, in sites with σ_y mirror-plane symmetry. Therefore, the symmetric stretching mode ν_1 is not expected in the cross-polarized B_{1g} and B_{2g} spectra. In phases III and IV, the crystal does not present the σ_y mirror plane and therefore at least one ν_1

TABLE II. Correlation diagram for the internal modes for the commensurate phase III of Cs_2HgBr_4.

point group of the free molecule	site group	factor group	internal modes
T_d	C_1	C_{2h}	
A_1 (ν_1)		A_g (x^2, y^2, z^2, yz)	$\nu_1, 2\nu_2, 3\nu_3, 3\nu_4$, 3lib, 3ext
E (ν_2)	A	B_g (xy, xz)	$\nu_1, 2\nu_2, 3\nu_3, 3\nu_4$, 3lib, 3ext
T_1 (lib.)		A_u (x)	$\nu_1, 2\nu_2, 3\nu_3, 3\nu_4$, 3lib, 3ext
T_2 (ν_3, ν_4, ext.)		B_u (y, z)	$\nu_1, 2\nu_2, 3\nu_3, 3\nu_4$, 3lib, 3ext

TABLE III. Correlation diagram for the internal modes for the commensurate phase IV of Cs$_2$HgBr$_4$.

point group of the free molecule	site group	factor group	internal modes
T_d	C_1	C_i	
A_1 (ν_1)		A_g (x^2, y^2, z^2, yz)	$2\nu_1$, $4\nu_2$, $6\nu_3$, $6\nu_4$, 6lib, 6ext
E (ν_2)	A		
T_1 (lib.)		A_u (xy, xz, x, y, z)	$2\nu_1$, $4\nu_2$, $6\nu_3$, $6\nu_4$, 6lib, 6ext
T_2 (ν_3, ν_4, ext.)			

mode is expected in each cross-polarized spectrum. Moreover, due to the lowering of the crystal symmetry with decreasing temperature, a large number of internal modes is expected in all spectra, as shown in Tables II and III.

There are different kinds of theoretical models which deal with the Raman activity in incommensurate structures and all of them predict the appearance of extra internal modes below the incommensurate phase transition.[14,15] According to the superspace description,[14] six new modes of A_g and B_{2g} symmetries, and 12 new modes of B_{1g} and B_{3g} symmetries are expected below T_I, considering that the incommensurate phase of Cs$_2$HgBr$_4$ has P^{Pnma}_{1ss} symmetry like as the K$_2$SeO$_4$-type compounds.

IV. RESULTS AND DISCUSSION

The ν_1 and ν_3 stretching internal modes in Cs$_2$HgBr$_4$ have their frequencies in the range 150–200 cm^{-1}. The ν_2

and ν_4 bending modes appear in the spectra below 85 cm^{-1} and are overlapped with the external modes due to the large mass of the HgBr$_4^{-2}$ tetrahedra. Figure 1 shows the room-temperature Raman spectra for different scattering geometries, which allow us to investigate all the Raman-active stretching modes (ν_1 and ν_3). The ν_1 modes are the most intense and have their frequencies at about 179 cm^{-1}. The peaks at about 160 and 185 cm^{-1} are associated with the ν_3 modes. The assignment of these modes were confirmed by a recent infrared study of Cs$_2$HgBr$_4$.[16]

Analysis of the ν_1-peak

The first interesting experimental result obtained concerns the observation of forbidden modes in some spectra. According to the factor-group analysis of Table I, a ν_1 mode with B_{1g} and B_{3g} symmetry is not expected if the HgBr$_4^{2-}$ tetrahedra are on a σ_y mirror plane. However, one ν_1 mode is always observed in the cross-polarized (xy) and (yz) spectra, which display the B_{1g} and B_{3g} modes, respectively, as shown in Figs. 1(e) and 1(f). Care was taken to be sure that these extra lines are not due to a crystal misorientation or leakage effects; the orientation of the crystallographic axes was systematically checked by x-ray diffraction.

The observation of the ν_1 mode in the cross-polarized (xy) and (yz) spectra can be explained if we consider that

FIG. 1. Room-temperature Raman spectra of Cs$_2$HgBr$_4$ showing the bands associated with the internal stretching modes for six different scattering geometries. (a) $y(xx)\bar{y}$, (b) $z(yy)\bar{z}$, (c) $x(zz)\bar{x}$, (d) $y(xz)\bar{y}$, (e) $z(xy)\bar{z}$, (f) $x(yz)\bar{x}$.
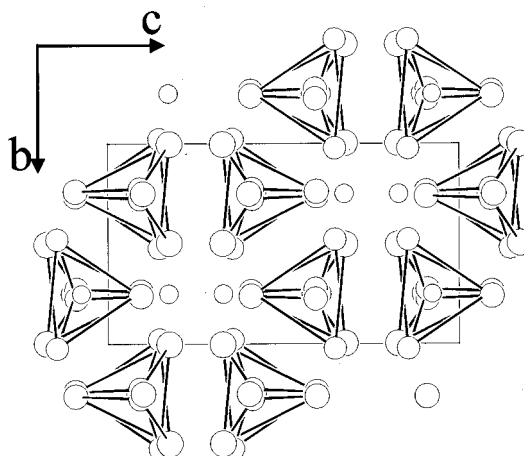
FIG. 2. Projection along the a axis of the disordered room-temperature structure of Cs$_2$HgBr$_4$.
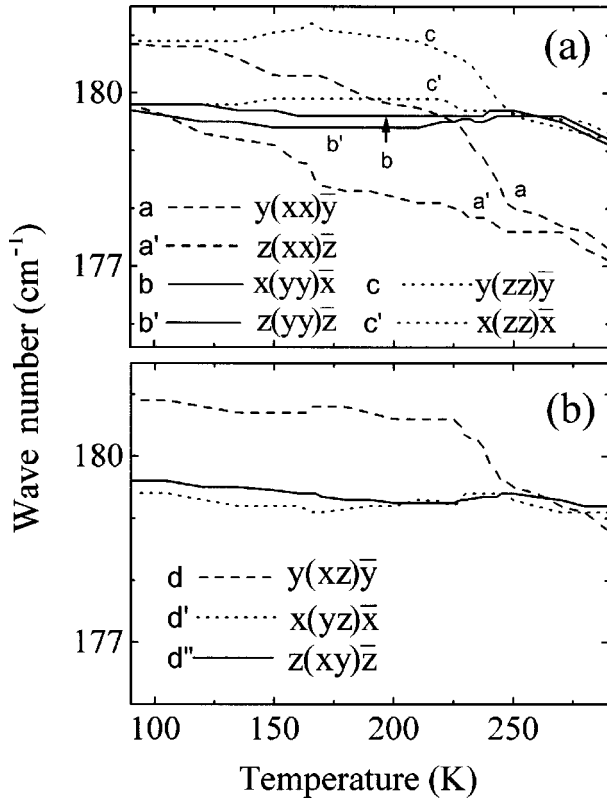
FIG. 3. Temperature dependence of the frequency of the peak associated with the ν_1 mode in nine different backscattering geometries.

the tetrahedra are not on the σ_y mirror plane of the *Pnma* structure. A recent x-ray-diffraction experiment[17] showed that the room-temperature structure of Cs_2HgBr_4 is better described by an orientational disordered model, illustrated in Fig. 2. In this model the tetrahedra are slightly deviated from the σ_y mirror plane, but the average structure presents *Pnma* symmetry. It must be emphasized that the observation of forbidden internal modes above T_I is a very common feature in K_2SeO_4-type compounds,[18–22] and led several authors to come to the same conclusion concerning the tetrahedra orientational disorder.

Let us now discuss the diagonally polarized (xx), (yy), and (zz) spectra. According to the group theory analysis three stretching modes with A_g symmetry (one ν_1 and two ν_3) are expected at room temperature. The spectra shown in Figs. 1(a), 1(b), and 1(c) corresponding to (xx), (yy), and (zz) configurations are quite different. The three predicted modes are clearly observed only in the (zz) spectra [Fig. 1(c)]. For the (xx) spectra we can observe the ν_1 mode and the low-frequency ν_3 mode [Fig. 1(a)]. On the other hand, only the ν_1 and the high-frequency ν_3 modes are present in the (yy) spectra [Fig. 1(b)].

The bands associated with the stretching modes were fitted by a sum of Lorentzian curves, as shown in Figs. 1(a), 1(b), and 1(c). In all cases, the ν_1 mode is the most intense one and the frequency of the associated peak can be determined with a precision better than ± 0.3 cm^{-1}. Since only one ν_1 and two ν_3 modes are expected in the diagonally polarized spectra, the bands shown in Figs. 1(a), 1(b), and 1(c) should be fitted using only three distinct frequencies.

Surprisingly, we could not fit these bands with only three distinct frequencies since the frequency of the peaks associated with the ν_1 mode depends on the scattering geometry of the diagonally polarized spectra. Figure 3(a) shows the temperature dependence of the frequency of the peak associated with the ν_1 mode in six different diagonally polarized spectra, which allow the observation of the A_g phonons propagating along the three crystallographic directions. Note that the frequency of the peak associated with the A_g-symmetry ν_1 mode depends on the spectra polarization, that is, the frequency of the ν_1 peak observed in the (xx) spectra (curves a and a') is smaller than those observed in the (yy) and (zz) spectra (curves b, b', c, c'). This frequency shift is about 2 cm^{-1} at room temperature, and it is much greater than the precision in the determination of the frequency peaks. On the other hand, at very low temperature ($T \sim 90$ K) the frequency of the ν_1 peak depends on the phonon propagation direction, that is, the peaks associated with the modes propagating along the y direction (curves a and c) have frequencies larger than those propagating along the x and z directions (curves a', b, b', c'). The same behavior is observed in Fig. 3(b) for the cross-polarized spectra. In the intermediate cases (phase II and III) the frequency of the ν_1 peak depends both on the spectra polarization and the phonon propagation direction.

Let us now analyze the dependence of the ν_1 peak frequency on the spectra polarization. This anomalous behavior was already verified in a very precise Raman study of K_2SeO_4 reported by Katkanant, Hardy, and Ullman.[21] They observed that the frequency of a given line in the A_g symmetry can be different in (xx), (yy), and (zz) spectra and ascribed this result to a "smearing" of the effective orthorhombic crystal caused by slightly random misorientations of the various tetrahedra groups. As previously discussed, the room-temperature phase of Cs_2HgBr_4 is characterized by an orientational disorder of the tetrahedra groups. The disordered model proposed by Pinheiro *et al.*[17] assumes that the tetrahedra rotations occurs about the pseudohexagonal x axis. Moreover, Dmitriev *et al.*[12] observed in the low-frequency Raman spectra of Cs_2HgBr_4 a relaxation wing associated with orientational jumps, which is absent in the (xx) spectra and concluded that the relaxation excitation is polarized. All these results lead us to the following qualitative conclusion: the ν_1 mode with symmetry A_g is coupled to the relaxation mode associated with the orientational disorder and the coupling shifts the frequency of the peak associated with the ν_1 mode. The strength of the coupling is not isotropic since rotation occurs preferentially about the x axis. Therefore, the shift in the frequency of the ν_1 peak observed in the (xx) spectra is different from the value observed in the (yy) and (zz) spectra.

Figure 4 shows the temperature dependency of $\omega_{b'} - \omega_{a'}$, where $\omega_{b'}$ and $\omega_{a'}$ are the frequencies of the ν_1 peaks observed in the $z(yy)\bar{z}$ and $z(xx)\bar{z}$. We can observe two discontinuous decreases in this curve, the first one at the incommensurate phase transition ($T_I = 245$ K), and the second one at about $T_{L1} = 165$ K, which corresponds to the III-IV transition. Below T_{L1}, the shift $\omega_{b'} - \omega_{a'}$ tends practically to zero, as it would be expected from the group theory analysis. Figure 5 shows the temperature dependence of the
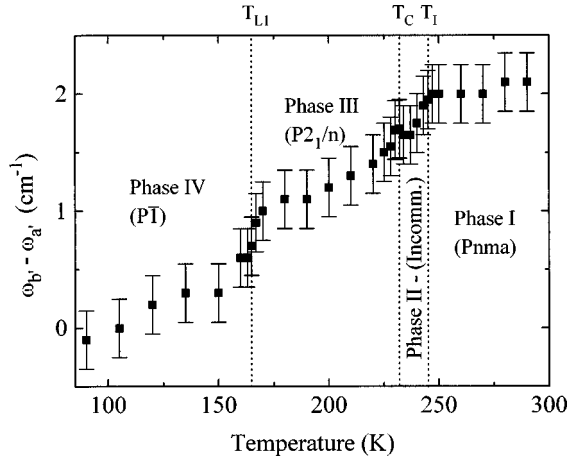
FIG. 4. Temperature dependence of $\omega_{b'}^2 - \omega_{a'}^2$, where $\omega_{b'}$ and $\omega_{a'}$ are the frequencies of the ν_1 modes observed in $z(yy)\bar{z}$ and $z(xx)\bar{z}$ spectra, respectively.

FIG. 6. Temperature dependence of $\omega_a^2 - \omega_{a'}^2$, where ω_a and $\omega_{a'}$ are the frequencies of the ν_1 peaks observed in the $y(xx)\bar{y}$ and $z(xx)\bar{z}$ spectra.

damping constants of the internal stretching modes. Note that these curves present a similar behavior of that shown in Fig. 4, that is, discontinuous decreases at $T_I = 245$ K and $T_{L1} = 165$ K. In this sense, the orientational disorder start to decrease below the incommensurate phase transition and practically disappears in the ordered phase IV ($T < 165$ K). This interpretation agrees with the low-frequency Raman results,[12] in which a relaxation mode, ascribed to the existence of small-angle orientational jumps of the $HgBr_4^{2-}$ groups, was observed at high temperature and disappeared upon the transition to phase IV.

Let us now discuss the dependence of the ν_1-peak frequency on the phonon propagation direction. Figure 3 shows that, below T_I, the modes propagating along the y direction (curves a, c and d) have their frequencies larger than those propagating along the x and z directions (curves a', b, b', c', d' and d''). This frequency splitting is similar to a TO-LO splitting for a polar mode if one considers that the
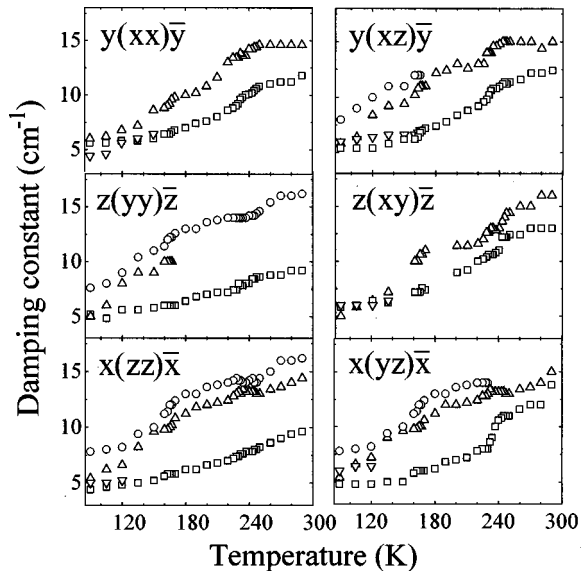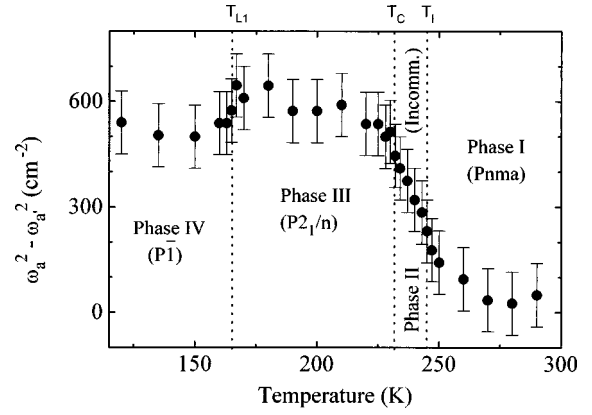
mode propagating along y is longitudinal (LO) and those propagating along x and z are transversal (TO). The higher value of the frequency of the modes propagating in the y direction is related to the existence of a macroscopic electric field in this direction, that increases the restoring forces, increasing their frequencies. The polar character of this modes can be given by its effective charge which is proportional to $\omega_{LO}^2 - \omega_{TO}^2$. Figure 6 shows the temperature dependence of $\omega_a^2 - \omega_{a'}^2$, where ω_a and $\omega_{a'}$ are the frequencies of the ν_1 modes observed in the $y(xx)\bar{y}$ and $z(xx)\bar{z}$ spectra, respectively. Therefore, the polar character of this mode appears at T_I, increases in the incommensurate phase and remains constant below the lock-in phase transition at T_C. However, it is well established that the low-temperature structural phases are centrosymmetric and therefore, according to the group-theory predictions, the polar modes are not Raman active. The reason of this intriguing result is not yet clear. A possible explanation for this result is related to the existence of domain walls. Notice that the symmetry breaking occurring from phase I to phase III gives rise to two types of twin domains at low temperature, which have already been observed by x-ray diffraction.[17] There are, in principle, three possible types of domain wall separating these twin domains, that is, walls perpendicular to the x, y, and z directions.

Let us now analyze the symmetry of these types of domain walls. The point group of phase I has eight symmetry elements ($D_{2h} = \{E, C_{2x}, C_{2y}, C_{2z}, i, \sigma_x, \sigma_y, \sigma_z\}$) and the phase III point group C_{2h} has the four symmetry elements ($C_{2h} = \{E, C_{2x}, i, \sigma_x\}$). Therefore, the two types of domain states are related between each other by the symmetry elements that are lost at the phase transition, that is, S

FIG. 5. Temperature dependence of the damping constants of the internal stretching modes in Cs_2HgBr_4 for six different scattering geometries. $\square = \nu_1$; $\triangle = \nu_3$; $\bigcirc = \nu_3'$; $\nabla = \nu_3''$.

TABLE IV. Symmetry elements and point groups of the three possible domain walls in phase III of Cs_2HgBr_4.

direction normal to the domain wall	symmetry elements of the domain wall	point group of the domain wall
x	$E, C_{2x}, C_{2y}, C_{2z}$	D_2
y	$E, C_{2z}, \sigma_x, \sigma_y$	$C_{2v}(z)$
z	$E, C_{2y}, \sigma_x, \sigma_z$	$C_{2v}(y)$
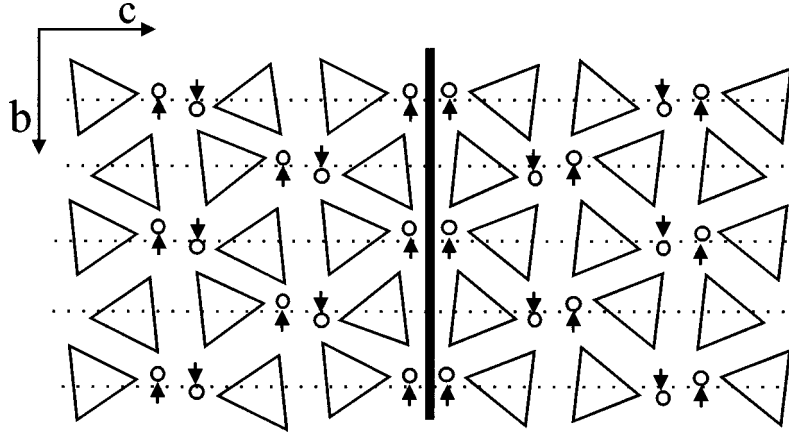
FIG. 7. Schematic projection of the phase III structure of Cs_2HgBr_4 along the *a* axis showing two domains separated by a domain wall perpendicular to the *z* direction. The arrows show the displacement of the cesium ions. The domain wall carries a polarization along the *y* direction.

$=\{C_{2y},C_{2z},\sigma_y,\sigma_z\}$. The point group of a given type of domain wall separating two regions 1 and 2 is formed by the symmetry elements of C_{2h} that do not interchange regions 1 and 2 and by the symmetry elements of S that interchange 1 and 2. Consider, for example, a domain wall perpendicular to the *z* direction. The point group of this domain wall is $F^{(z)}=\{E,C_{2y},\sigma_x,\sigma_z\}$. Table IV shows the symmetry elements and the point groups of the three types of domain walls. Notice that the point groups associated with the domain walls perpendicular to the *y* and *z* directions are polar, the polar axis being along the *z* and *y* directions, respectively. Therefore, in spite of the fact that each domain has a centrosymmetric structure, the domain walls perpendicular to *y* and *z* can present a macroscopic polarization.

As pointed out in Sec. II, the Cs_2HgBr_4 crystals present an easy cleavage plane perpendicular to the *z* direction. The bonding between atoms in that direction is weaker than in other directions. This can be seen in Fig. 7 which clearly shows an empty layer perpendicular to *z*, between two neighboring $HgBr_4$ tetrahedra. Therefore, the domain wall perpendicular to *z* is of lower energy than the walls perpendicular to *x* and *y* since it is easier to accommodate two domains in this plane. Figure 7 shows that the displacement of the cesium ions [Cs(1)] occurs principally along the *y* direction creating a local electric dipole. Since the cesium ions in the unit cell move in opposite senses, the net electric dipole of the unit cell is null. However, in a domain wall perpendicular to the *z* direction, the cesium atoms move in the same direction. In this case, there is a macroscopic polarization along the *y* direction, in accordance with the group-theory analysis of the domain wall discussed above.

In summary, a possible explanation for the TO-LO splitting presented in Fig. 6 is the existence of a macroscopic polarization along the *y* direction associated with a layered structure of domains perpendicular to the *z* direction. The polarization is due to the displacement of the cesium atoms from the σ_y mirror plane. The increasing of the TO-LO splitting in the incommensurate phase probably reflects the correlation between the cesium ion displacements with the onset of the tetrahedra orientational ordering, that occurs at T_I.

The appearance of new modes at low temperature

As discussed in Sec. III, there are different theoretical models that predict the appearance of new internal modes

below the incommensurate phase transition in A_2BX_4 compounds.[14,15] In a Raman study of Rb_2ZnBr_4, Rasing *et al.*[14] observed the appearance of three new internal modes below T_I, while 16 were expected according to their theoretical model. The appearance of new internal modes has also been observed in K_2SeO_4, Rb_2ZnCl_4, and K_2ZnCl_4.[23-25]

Figure 8 shows the temperature dependence of all stretching internal mode frequencies between 90 and 290 K. Note that no extra bands appear below the incommensurate phase transition in Cs_2HgBr_4, in disagreement with the predictions of the superspace approach displayed in Table II.[14] Dimitriev *et al.*[12] came to the same conclusion in their Raman study of Cs_2HgBr_4. We performed a careful fit of each spectra in order to observe a possible effect of the incommensurability on the line shape of the bands. The line shape analysis showed that all spectra could be fitted as a sum of Lorentzian lines, exactly as in the room-temperature structure, leading us to the conclusion that no extra bands appear in the incommensurate phase of Cs_2HgBr_4.
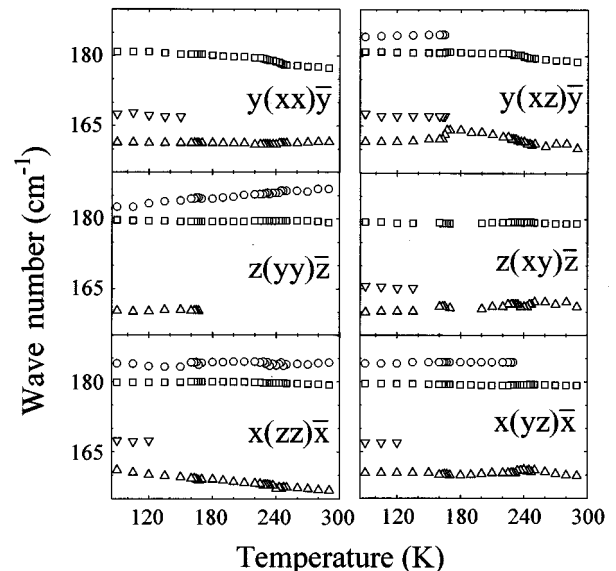
FIG. 8. Temperature dependence of the frequencies of the internal stretching modes in Cs_2HgBr_4 for six different scattering geometries. $\square = \nu_1$; $\triangle = \nu_3$; $\bigcirc = \nu_3'$; $\nabla = \nu_3''$.
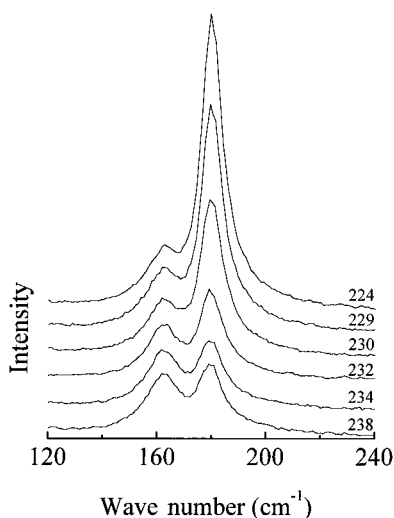
FIG. 9. Temperature dependence of the $x(yz)\bar{x}$ Raman spectrum showing the bands associated with the internal stretching modes.

It must be observed that the appearance of additional modes in the incommensurate phase of K_2SeO_4-type compounds is compatible with the triplication of the unit cell which occurs in the commensurate phase. The absence of extra internal modes in the incommensurate phase of the Cs_2HgBr_4 should be related to the fact that there is no superstructure in the commensurate phase, below T_C. Another possible explanation is the important disorder effects that partly obscure the validity of the theoretical predictions.

Figure 9 shows the temperature dependence of the $x(yz)\bar{x}$ spectra between 224 and 238 K. The lock-in phase transition at 232 K manifests itself by the increase of the intensity of the ν_1 mode and the appearance of a new mode (see Fig. 8). Note that now, the ν_1 mode is allowed by group theory in the (xy) and (yz) spectra. The particular increase in the ν_1 peak intensity in the (yz) spectra can be related to the fact that (yz) quadratic function belongs to the identical representation below the lock-in transition (see Table II).

On further cooling, a phase transition is observed at about 165 K, in agreement with different experimental studies. Figure 8 shows the appearance of additional internal stretching modes in practically all scattering geometries. The appearance of those modes is ascribed to the decrease of the point-group symmetry, as shown in Table III.

V. CONCLUSION

It is well known that the sequence of phase transitions in the A_2BX_4 compounds is related to the orientation and dis-

order of the BX_4 tetrahedra. In particular, the incommensurate modulation is associated with the orientation of the BX_4 groups. The main conclusions of this study were obtained from the detailed analysis of the totally symmetrical stretching mode (ν_1). At room temperature, the frequency of the peak associated with the ν_1 mode observed in the (xx) spectra is smaller than its value in the (yy) and (zz) spectra. Moreover, its frequency does not depend on the phonon propagation direction. This difference is ascribed to the orientational disorder of the $HgBr_4^{2-}$ tetrahedra, which couples the ν_1 mode with a relaxation mode associated with the orientational jumps of the tetrahedra and shifts the frequency of the peak associated with the ν_1 modes. The strength of the coupling is not isotropic, due to the fact that the rotations of the tetrahedra groups occurs preferentially around the x axis. Probably this kind of behavior is common, in a greater or lesser extent, to the other A_2BX_4 incommensurate compounds since they exhibit orientational disorder effects above T_I. The difference in the frequency of the peaks associated with the ν_1 mode observed in different diagonally polarized spectra presents a discontinuous decrease at the incommensurate phase transition and jumps practically to zero at about $T_{L1} = 165$ K (III-IV phase transition). These discontinuities are also observed in the temperature dependence of the damping constants, suggesting that the orientational disorder starts to decrease below T_I and disappears only below the III-IV phase transition.

On the other hand, a TO-LO splitting of the ν_1 mode appears at T_I, increases in the incommensurate phase and remains practically constant below T_C. The polar character of this mode below T_C is incompatible with the centrosymmetric structures proposed for the low-temperature phases. Probably, this result is related to the existence of a macroscopic electric field along the y direction associated with layered structure of domains perpendicular to z direction.

[1] D. Altermatt, H. Arend, V. Gramlich, A. Niggli, and W. Petter, Mater. Res. Bull. **14**, 1391 (1979).

[2] S. Plesko, R. Kind, and H. Arend, Phys. Status Solidi A **61**, 87 (1980).

[3] S. Plesko, V. Dvorak, R. Kind, and A. Treindl, Ferroelectrics **36**, 331 (1981).

[4] D. Altermatt, H. Arend, V. Gramlich, A. Niggli, and W. Petter,

Acta Crystallogr., Sect. B: Struct. Sci. **40**, 347 (1984).

[5] A. V. Bondar, S. M. Ryabchenko, and A. Yu. Khalakhan, Sov. Phys. Solid State **30**, 1315 (1988).

[6] A. A. Boguslavskii, Yu. N. Ivanov, A. I. Krieger, A. K. Moskalev, V. I. Pakhomov, and R. Sh. Lotfullin, Phys. Status Solidi B **161**, K49 (1990).

[7] A. V. Kityk, O. M. Mokry, V. P. Soprunyuk, and O. G. Vlokh, J.

Phys.: Condens. Matter **5**, 5189 (1993).

[8] O. G. Vlokh, V. S. Zhmurko, I. I. Polovinko, and S. A. Sveleba, Sov. Phys. Solid State **33**, 1758 (1991).

[9] O. G. Vlokh, A. V. Kityk, O. M. Mokryi, V. V. Kirilenko, I. D. Olekseyuk, and S. A. Piroga, Sov. Phys. Solid State **31**, 901 (1989).

[10] O. G. Vlokh, V. G. Gribik, A. V. Kityk, O. M. Mokryi, I. D. Olekseyuk, and S. A. Piroga, Sov. Phys. Crystallogr. **35**, 873 (1990).

[11] V. V. Petrov, A. Yu. Khalakhan, V. G. Pitsyuga, and V. E. Yachmenev, Sov. Phys. Solid State **30**, 906 (1988).

[12] V. P. Dmitriev, Yu. I. Yuzyuk, Yu. I. Durnev, L. M. Rabkin, E. S. Larin, and V. I. Pakhomov, Sov. Phys. Solid State **31**, 770 (1989).

[13] Different conventions are used to label the crystal axes, and, therefore, we have to be careful when comparing different publications.

[14] Th. Rasing, P. Wyder, A. Janner, and T. Janssen, Phys. Rev. B **25**, 7504 (1982).

[15] H. Poulet and R. M. Pick, in *Incommensurate Phases in Dielectrics*, edited by R. Blinc and A. P. Levanyuk (North-Holland, Amsterdam, 1986), pp. 315.

[16] A. Jório, P. Echegut, N. L. Speziali, and M. A. Pimenta (unpublished.)

[17] C. B. Pinheiro, A. Jorio, M. A. Pimenta, and N. L. Speziali, Acta Crystallogr. B (to be published.)

[18] N. E. Massa, F. G. Ullman, and J. R. Hardy, Phys. Rev. B **27**, 1523 (1983).

[19] I. Noiret, Y. Guinet, and A. Hedoux, Phys. Rev. B **52**, 13 206 (1995).

[20] V. I. Torgashev, Yu. I. Yuzyuk, F. Smutný, P. Vanek, and B. Brezina, Phys. Status Solidi B **154**, 777 (1989).

[21] V. Katkanant, J. R. Hardy, and F. G. Ullman, Ferroelectrics **82**, 185 (1988).

[22] F. G. Ullman, Ferroelectrics **117**, 245 (1991).

[23] P. Echégut, F. Gervais, and N. E. Massa, Phys. Rev. B **31**, 581 (1985).

[24] P. Echégut, F. Gervais, and N. E. Massa, Phys. Rev. B **30**, 6039 (1984).

[25] I. Noiret, A. Hedoux, Y. Guinet, and M. Foulon, Europhys. Lett. **22**, 265 (1993).